Measuring the Invasiveness of High-Impedance Probes

Uwe Arz[1*], Pavel Kabos[2], and Dylan Williams[2]
[1]Physikalisch-Technische Bundesanstalt (PTB), Bundesallee 100, 38116 Braunschweig, Germany
[2]National Institute of Standards and Technology (NIST), 325 Broadway, Boulder, CO 80305, USA
E-mail : Uwe.Arz@PTB.de Phone :++49-531-762-2297

Abstract

We use on-wafer measurements to characterize the invasiveness of high-impedance probes over a broad frequency range. We show that a two-port representation characterizing the invasiveness of the probe can also be determined from a calculation of the probe's load impedance, which is derived from a separate characterization of the high-impedance probe.

Introduction

In this paper we describe a method for characterizing the invasiveness of a high-impedance probe (HIP) used to perform measurements in coplanar waveguide (CPW). We quantify the influence of the high-impedance probe with a two-port scattering parameter representation, which we call the "invasiveness error box". We demonstrate that this error box can also be calculated from the load impedance presented by the high-impedance probe in the CPW. Finally, we show that the calculated invasiveness error box may be used to predict the loading of the CPW by the high-impedance probe.

We have recently introduced two methods of characterizing the reflection and transmission of high-impedance probes [1], both of which give equivalent results. We then applied one of the high-impedance-probe characterization procedures of [1], together with a frequency-domain mismatch correction scheme, to the calibration of time-domain waveform measurements performed with the high-impedance probe [2]. Since commercially available high-impedance probes are suitable for fine-pitch applications, they may play a role as an alternative to traditional handheld oscilloscope probes for internal node testing in today's high-density circuit environments.

Here, we focus on the invasiveness of the high-impedance probe. We determine an invasiveness error box both from measurement and calculation, the latter explaining the high-impedance probe's influence from a more physical point of view.

On-wafer invasiveness measurement

The measurement setup used for our investigations is sketched in Fig. 1. We used a vector network analyzer (VNA) and two conventional ground-signal-ground (GSG) microwave probes to contact and measure the scattering parameters of our CPW test structures. Some of the measurements were intentionally disturbed by the presence of the high-impedance probe, which touched down on the signal conductor of the CPW in the middle of the length of the CPW. Although the high-impedance probe was provided with an additional ground tip that could have been placed on either of the CPW grounds, we did not make use of this additional grounding capability. The high-impedance probe had a 950 Ω resistor built into the tip to reduce invasiveness on the device under test (DUT). In order to mimic a typical measurement environment, we terminated the high-impedance probe with a broadband coaxial 50 Ω load.

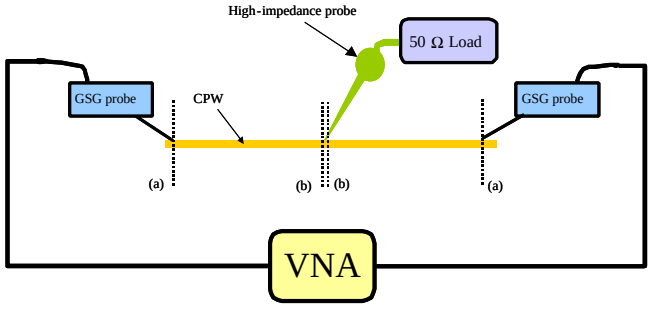

Fig. 1. Experimental setup.

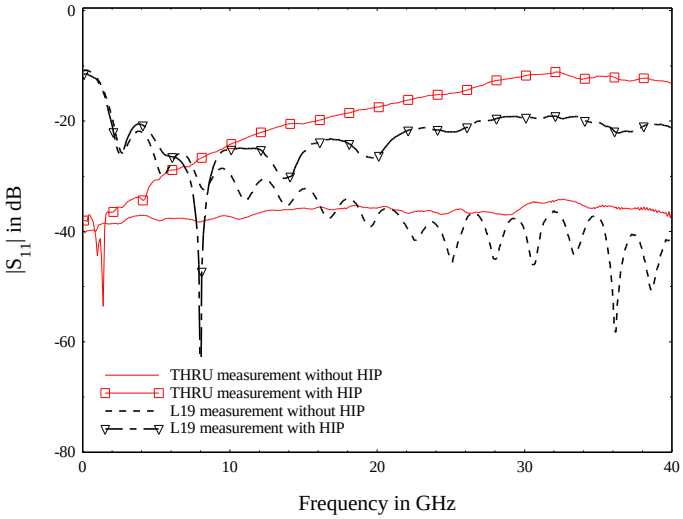

Fig. 2. Influence of the high-impedance probe on probe-tip calibrated measurements of a CPW THRU standard and 19 mm long CPW line standard.

We started by performing a first-tier Multiline Thru-Reflect-Line (TRL) calibration [3] with a 50 Ω reference impedance [4]. The on-wafer calibration artifacts we used consisted of a symmetric CPW reflect and CPW transmission lines with lengths of 0.5, 2.635, 3.7, 7.065, and 20.195 mm. The initial reference plane of the calibration in the middle of

[*] U. Arz was a visiting post-doctoral research associate from the University of Hannover, Germany, at NIST, Boulder, CO.

the 0.5 mm long Thru standard was moved close to the probe tips (position labeled (a) in Fig.1).

Fig. 2 shows measurements of two CPW line standards corrected to this probe-tip reference plane, both with and without the high-impedance probe touching down on the signal conductor in the middle of the waveguide. The curves labeled with THRU and L19 correspond to the 0.5 mm and to the 20.195 mm long line, respectively. The magnitude of the reflection coefficient S_{11} clearly illustrates the high-impedance probe's loading effect on the waveguide.

In order to isolate the high-impedance probe's invasiveness properties, we moved the calibration reference plane from position (a) in Fig. 1 to position (b), which is close to the tip of the high-impedance probe. With this new reference plane position we calibrated the measurement of the 0.5 mm long line with the high-impedance probe touching down. As a result of this procedure we obtained a 2-port S-parameter representation of the disturbance introduced by the high-impedance probe, which we call the invasiveness error box. We used a standard S-to-Z transformation to investigate the measured impedance parameters Z_{ij} of this invasiveness error box (Fig. 3).

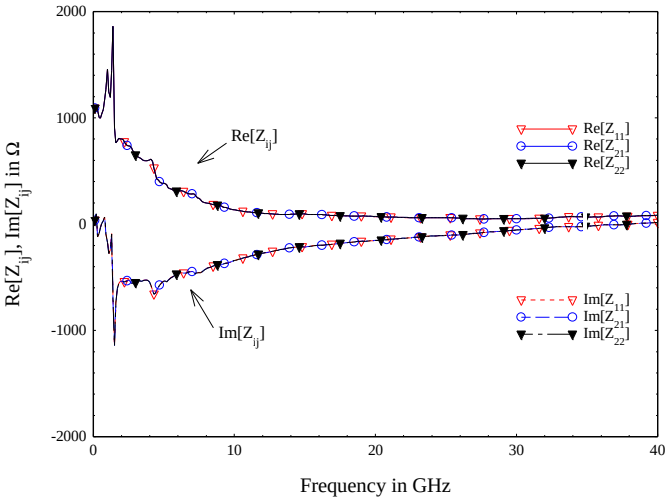

Fig. 3. Measured elements of the impedance matrix of the invasiveness error box.

Fig. 3 shows that all of the measured impedance parameters are virtually identical. A general equivalent-circuit model for reciprocal two ports [5], which also holds for the invasiveness error box, is shown in Fig. 4.

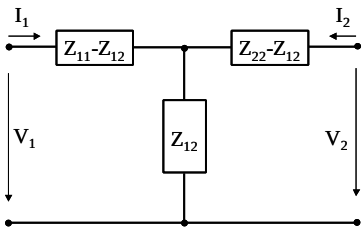

Fig. 4. General equivalent circuit model.

Together with the results of Fig. 3 we conclude that one single frequency-dependent shunt element with load impedance Z_{load} equal to Z_{ij} is sufficient to model the measured invasiveness error box. Also, from Fig. 3, we conclude that the high-impedance probe essentially introduces a capacitive loading to the circuit under test.

Calculation of invasiveness error box from the measured high-impedance-probe's scattering parameters

The load impedance Z_{load} can also be derived from the high-impedance-probe's scattering parameters S_{ij} determined with procedure A of [1]. Together with a measurement of the reflection coefficient of the coaxial load serving as the high-impedance-probe's termination, Γ_{term}, the input reflection at the high-impedance-probe's probe tip Γ_{load} can be determined as follows:

$$\Gamma_{load} = S_{11} + S_{12}S_{21}\frac{\Gamma_{term}}{1 - S_{22}\Gamma_{term}} \quad . \tag{1}$$

The conversion to the load impedance is straightforward:

$$Z_{load} = 50 \cdot \frac{1+\Gamma_{load}}{1-\Gamma_{load}} \quad . \tag{2}$$

Fig. 5 compares the load impedance determined by direct measurement (dashed lines) to the calculation using (1) and (2) (solid lines). Both values agree fairly well over the entire 40 GHz frequency range.

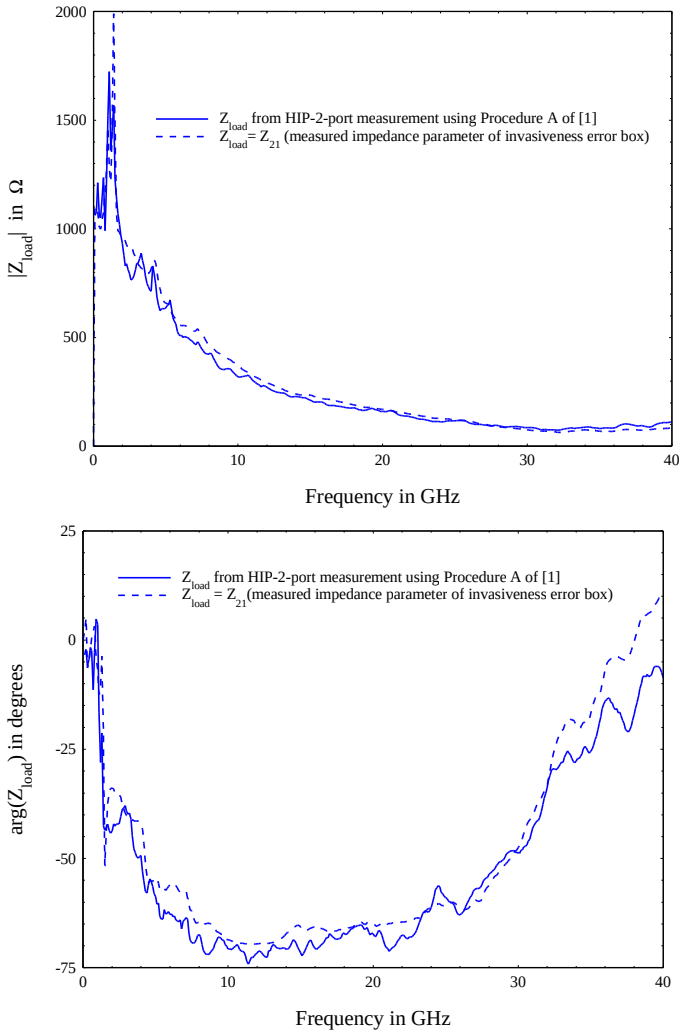

Fig. 5. Magnitude (top frame) and phase angle (bottom frame) of measured and calculated load impedance Z_{load}.

Calculating the DUT's behavior in presence of the HIP

In order to verify whether the invasiveness error box can be used to predict the behavior of the device under test when the high-impedance probe touches down, we compared first-tier corrected measurements of the CPW artifacts (transmission lines of different lengths) to calculations based on the model of Fig. 6.

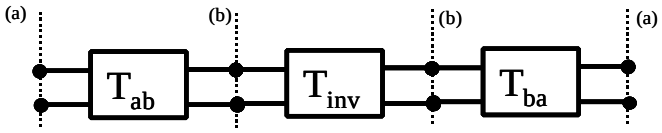

Fig. 6. Model of the CPW waveguide measurement in the presence of the high-impedance probe.

We modeled the CPW measurements corrected with respect to the probe-tip reference planes labeled (a) in Fig. 1 as a cascade of three transmission matrices $T_{CPW}=T_{ab}\ T_{inv}\ T_{ba}$. The transmission matrices T_{ab}, T_{inv}, and T_{ba} shown in Fig. 6 represent the left half of the CPW, the high-impedance probe's invasiveness error box, and the right half of the CPW. Here we determined the transmission matrix T_{inv} of the invasiveness error box from either the direct measurement or the calculation procedure described in the previous section.

In order to determine the transmission matrices T_{ab} and T_{ba}, we defined a second-tier Multiline-TRL calibration at reference plane (b). The relationship between the first-tier calibration at reference plane (a) and the second-tier calibration at reference plane (b) is given by a pair of error boxes that capture the electrical parameters of the section between the two reference planes (a) and (b). We set the matrices T_{ab} and T_{ba} to the two error boxes determined by this somewhat artificial two-tier calibration procedure.

Fig. 7 compares the first-tier corrected measurements of the reflection coefficient of the 0.5-mm long THRU standard and of the 20.195-mm long L19 standard to calculations based on the model of Fig. 6. When using the measured invasiveness error box, the calculation for the THRU standard (dashed line with squares) coincides with the overall first-tier corrected measurement (solid line), as expected. The calculation using the invasiveness error box determined via (1) and (2) (dashed line without markers) is also in good agreement for the given bandwidth of 40 GHz.

For the L19 CPW measurement, we cannot expect the calculation using T_{inv} from the direct invasiveness measurement (dashed line with triangles) to exactly coincide with the first-tier corrected measurement (solid line), since T_{inv} was determined using the THRU standard. However, the agreement is still fairly good. The same is true of the calculation using T_{inv} from the model of (1) and (2) (dashed line). This demonstrates that the error-box model of the probe's invasiveness is applicable to a variety of probing situations.

Similar agreement between measurement and calculations was obtained for the remaining scattering parameters of the CPWs, but is not shown here.

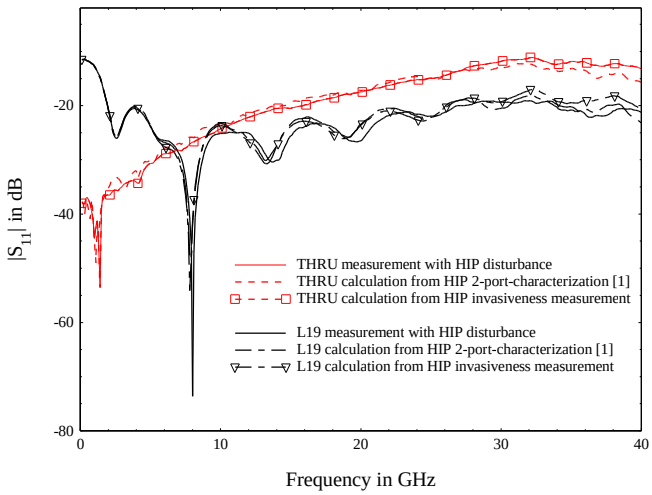

Fig. 7. Measured and calculated magnitudes of the reflection coefficient of the CPW standards THRU and L19.

Conclusions

We have introduced an on-wafer measurement procedure that characterizes the invasiveness of commercial high-impedance probes. The invasiveness of the probe can be either described by a frequency-dependent two-port representation, the invasiveness error box, or by the load impedance calculated from the reflection coefficient of the high-impedance probe terminated in a 50 Ω load. We have verified the accuracy of the invasiveness-error-box representation by comparing CPW measurements to calculations.

References

[1] U. Arz, H. Reader, P. Kabos, and D. F. Williams, "Wideband frequency-domain characterization of high-impedance probes," 58th ARFTG Conference Digest, San Diego, CA, USA, Nov. 2001.

[2] P. Kabos, H.C. Reader, U. Arz, and D. F. Williams, "Calibrated waveform measurement with high-impedance probes," IEEE Trans. Microwave Theory Tech., vol.51, no.2, pp. 530-535, Feb. 2003.

[3] R. B. Marks, "A multiline-method of network analyzer calibration," IEEE Trans. Microwave Theory Tech., vol. MTT-39, pp. 1205-1215, 1991.

[4] R.B. Marks and D.F. Williams, "Characteristic impedance determination using propagation constant measurement," IEEE Microwave Guided Wave Lett., vol. 1, no. 6, pp. 141-143, June 1991.

[5] S. Ramo, J. Whinnery, and T. van Duzer, "Fields and waves in communication electronics," 3rd edition, p. 538, John Wiley&Sons, 1994.